Similarly, for myometrial depth of invasion, the range was equally wide: from 72% to 97%.[7,8,10,11] The accuracy rate of IFS diagnosis in our study is included in the table, and it is well within the range of these past reports.

However, the complete accuracy rate of IFS diagnosis, namely, being correct for both the histopathology type and myometrial depth, was, unfortunately, only 56%. However, in our study, a frozen section analysis was performed on all the subtypes of endometrial cancer, and for the subgroup of serous papillary and clear cell tumors, the histological error rate of IFS diagnosis was previously reported to be as high as 70%.[12] Even if these specific tumor types are excluded from our results, the complete accuracy rate only improved from 56% to 62%.

We retrospectively found 2 reasons for the discrepancies for IFS diagnosis. One was the anticipated tissue sampling error, and the other was an interobserver problem, which means that on reexamination, there was no difference found in the diagnosis achieved by the IFS and the diagnosis made from the fixed slides when done by another pathologist in a blinded test.

As these data showed, we should be able to improve significantly on the accuracy rate achievable with IFS by making more slides, not only one site, to decrease the sampling error, and by observation of the IFS slides by 2 or more pathologists. In our facilities and also most of the facilities in Japan, only one pathologist would have observed operative tissues in usual. Similar factors responsible for the diagnostic inaccuracy from frozen sections have been extensively documented by others.[13,14] The most common causes are reported to be erroneous interpretation or difficulties associated with technical artifact introduced by the frozen section technique. Other causes for inaccuracy include the inadequate sampling error we encountered. However, although sampling errors can be decreased through multiple sections, severe time constraints must be managed, and it is important to leave some discriminating tissue for paraffin embedding.[13]

On the other hand, it should also be noted that we had only a 54% accuracy rate for MRI diagnosis for determining myometrial invasion as a preoperative diagnosis. In the literature, the accuracy rate of MRI was 85% to 89% for myometrial invasion.[15–17] Our 29% misdiagnosis rate for myometrial invasion by MRI was mainly between stages IA and IB and when using the previous FIGO staging system. Our accuracy rate for MRI staging is much higher, now that we are using the revised FIGO system. On the other hand, MRI provides higher accuracy than other imaging modalities, including transvaginal sonography and computed tomography in endometrial cancer.[18–20] Moreover, Kinkel et al[15] found that contrast-enhanced MRI performed significantly better than no enhanced MR imaging and US ($P < 0.002$) and showed a trend toward better results when compared with CT ($P = 0.18$) in the evaluation of myometrial invasion. In patients with a large uterine mass and a resultant a higher probability of lymph node metastasis, MRI or CT, and not US, should be used as the primary imaging modality. However, Nakao et al[21] say that ready application of conservative treatment or omission lymphadenectomy for probable patients with stage IA endometrial cancer should be avoided owing to the relatively low preoperative diagnostic efficacy of MRI.

In conclusion, we report on our accuracy rate of preoperative and intraoperative diagnosis when using the previous and now the revised FIGO staging systems in our facility. Although MRI is better at predicting myometrial invasion using the revised FIGO staging compared to the previous one, IFS would still need to be performed. Physicians could consider the preoperative evaluation to include endometrial curettage and imaging whether by ultrasound or CT scan but not necessarily MRI.

REFERENCES

1. The Writing Committee, on behalf of the ASTEC Study Group. Efficacy of systematic pelvic lymphadenectomy in endometrial cancer (MRC ASTEC trial): a randomized study. *Lancet.* 2009;373:125–136.
2. Creaseman WY, Morrow CP, Bundy BN, et al. Surgical pathologic spread patterns of endometrial cancer: a Gynecologic Oncology Group Study. *Cancer.* 1987;60:2035–2041.
3. Kilgore LC, Partridge EE, Alvarez RD, et al. Adenocarcinoma of the endometrium: survival comparisons of patients with and without pelvic node sampling. *Gynecol Oncol.* 1995;56:29–33.
4. Case AS, Rocconi RP, Straughn JM, et al. A prospective blinded evaluation of the accuracy of frozen section for the surgical management of endometrial cancer. *Obstet Gynecol.* 2006;108:1375–1379.
5. Todo Y, Kato H, Kaneuchi M, et al. Survival effect of para-aortic lymphadenectomy in endometrial cancer (SEPAL study): a retrospective cohort analysis. *Lancet.* 2010;375:1165–1172.
6. Kayikcioglu F, Boran N, Meydanli MM, et al. Is frozen-section diagnosis a reliable guide in surgical treatment of stage I endometrial carcinoma? *Acta Oncol.* 2002;41:444–446.
7. Fanning J, Tsukada Y, Piver MS. Intraoperative frozen section diagnosis of depth of myometrial invasion in endometrial adenocarcinoma. *Gynecol Oncol.* 1990;37:47–50.
8. Noumoff JS, Menzin A, Mikuta J, et al. The ability to evaluate prognostic variables on frozen section in hysterectomies performed for endometrial carcinoma. *Gynecol Oncol.* 1991;42:202–208.
9. Larson DM, Johnson K, Olson KA. Pelvic and para-aortic lymphadenectomy for surgical staging of endometrial cancer: morbidity and mortality. *Obstet Gynecol.* 1992;79:998–1001.
10. Zorlu CG, Kuscu E, Ergun Y, et al. Intraoperative evaluation of prognostic factors in Stage 1 endometrial cancer by frozen section: now reliable? *Acta Obstet Gynecol Scand.* 1993;72:382–385.
11. Malviya VK, Deppe G, Malone JM Jr, et al. Reliability of frozen section examination in identifying poor prognostic indicators in stage I endometrial adenocarcinoma. *Gynecol Oncol* 1989;34:299–304.
12. Shim JU, Rose PG, Reale FR, et al. Accuracy of frozen section diagnosis at surgery in clinical stage 1 and 2 endometrial carcinoma. *Am J Obstet Gynecol.* 1992;166:1335–1338.

13. Howanitz PJ, Hoffman GC, Zarbo RJ. The accuracy of frozen section diagnosis in 34 hospitals. *Arch Pathol Lab Med.* 1990;114:355–359.
14. Wang KG, Chen TC, Wang TY, et al. Accuracy of frozen section diagnosis in gynecology. *Gynecol Oncol.* 1998;70:105–110.
15. Kinkel K, Kaji Y, Yu KK, et al. Radiologic staging in patients with endometrial cancer: a meta-analysis. *Radiology.* 1999;212:711–718.
16. Tsuda H, Murata K, Kawabata M, et al. Preoperative assessment of myometrial invasion of endometrial cancer by magnetic resonance imaging and intrauterine ultrasonography with a high-frequency probe: a preliminary study. *J Ultrasound Med.* 1997;24:520–526.
17. Shibutani O, Joja I, Shiraiwa M, et al. Endometrial carcinoma: efficacy of thin section oblique axial magnetic resonance image for evaluating cervical invasion, *Abdom Imaging.* 1999;24:520–526.
18. Rockall AG, Meroni R, Sohaib SA, et al. Evaluation of endometrial carcinoma on magnetic resonance imaging. *Int J Gynecol Cancer.* 2007;17:188–196.
19. Barwick TD, Rockall AG, Barton DP, et al. Imaging of endometrial adenocarcinoma. *Clin Radiol.* 2006;61: 545–555.
20. Yamashita Y, Harada M, Sawada T, et al. Normal uterus and FIGO stage I endometrial carcinoma: dynamic gadolinium-enhanced MR imaging. *Radiology.* 1993;186:495–501.
21. Nakao Y, Yokoyama M, Hara K, et al. MR imaging in endometrial carcinoma as a diagnostic tool for the absence of myometrial invasion. *Gynecol Oncol.* 2006;102:343–347.

Published OnlineFirst July 7, 2011; DOI:10.1158/1078-0432.CCR-10-3176

Clinical Cancer Research

Targeting Src in Mucinous Ovarian Carcinoma

Koji Matsuo, Masato Nishimura, Justin N. Bottsford-Miller, et al.

Clin Cancer Res 2011;17:5367-5378. Published OnlineFirst July 7, 2011.

Published OnlineFirst July 7, 2011; DOI:10.1158/1078-0432.CCR-10-3176

Clinical Cancer Research

Targeting Src in Mucinous Ovarian Carcinoma

Koji Matsuo[1,5], Masato Nishimura[1,6], Justin N. Bottsford-Miller[1], Jie Huang[1], Kakajan Komurov[2], Guillermo N. Armaiz-Pena[1,3], Mian M. K. Shahzad[1,7], Rebecca L. Stone[1], Ju Won Roh[1], Angela M. Sanguino[1], Chunhua Lu[1], Dwight D. Im[8], Neil B. Rosenshien[8], Atsuko Sakakibara[9], Tadayoshi Nagano[9], Masato Yamasaki[10], Takayuki Enomoto[11], Tadashi Kimura[11], Prahlad T. Ram[2], Kathleen M. Schmeler[1], Gary E. Gallick[3], Kwong K. Wong[1], Michael Frumovitz[1], and Anil K. Sood[1,3,4]

Abstract

Purpose: Mucinous ovarian carcinomas have a distinct clinical pattern compared with other subtypes of ovarian carcinoma. Here, we evaluated (i) stage-specific clinical significance of mucinous ovarian carcinomas in a large cohort and (ii) the functional role of Src kinase in preclinical models of mucinous ovarian carcinoma.

Experimental Design: A total of 1,302 ovarian cancer patients including 122 (9.4%) cases of mucinous carcinoma were evaluated for survival analyses. Biological effects of Src kinase inhibition were tested using dasatinib-based therapy in a novel orthotopic mucinous ovarian cancer model (RMUG-S-ip2).

Results: Patients with advanced-stage mucinous ovarian cancer had significantly worse survival than those with serous histology: median overall survival, 1.67 versus 3.41 years, $P = 0.002$; median survival time after recurrence of 0.53 versus 1.66 years, $P < 0.0001$. Among multiple ovarian cancer cell lines, RMUG-S-ip2 mucinous ovarian cancer cells showed the highest Src kinase activity. Moreover, oxaliplatin treatment induced phosphorylation of Src kinase. This induced activity by oxaliplatin therapy was inhibited by concurrent administration of dasatinib. Targeting Src with dasatinib *in vivo* showed significant antitumor effects in the RMUG-S-ip2 model but not in the serous ovarian carcinoma (SKOV3-TR) model. Combination therapy of oxaliplatin with dasatinib further showed significant effects on reducing cell viability, increasing apoptosis, and *in vivo* antitumor effects in the RMUG-S-ip2 model.

Conclusions: Our results suggest that poor survival of women with mucinous ovarian carcinoma is associated with resistance to cytotoxic therapy. Targeting Src kinase with a combination of dasatinib and oxaliplatin may be an attractive approach for this disease. *Clin Cancer Res; 17(16); 5367–78. ©2011 AACR.*

Authors' Affiliations: Departments of [1]Gynecologic Oncology and Reproductive Medicine, [2]Systems Biology, and [3]Cancer Biology, MD Anderson Cancer Center, and [4]Center for RNA Interference and Non-Coding RNA, University of Texas, Houston, Texas; [5]Department of Obstetrics and Gynecology, Norris Comprehensive Cancer Center, University of Southern California, Los Angeles, California; [6]Department of Obstetrics and Gynecology, University of Tokushima, Tokushima, Japan; [7]Department of Obstetrics and Gynecology, University of Wisconsin School of Medicine and Public Health, Madison, Wisconsin; [8]The Gynecologic Oncology Center, Mercy Medical Center, Baltimore, Maryland; [9]Department of Obstetrics and Gynecology, Kitano Hospital; [10]Department of Obstetrics and Gynecology, Osaka Rosai Hospital; and [11]Department of Obstetrics and Gynecology, Osaka University Graduate School of Medicine, Osaka, Japan

Note: Supplementary data for this article are available at Clinical Cancer Research Online (https://clincancerres.aacrjournals.org/).

Corresponding Author: Anil K. Sood, Departments of Gynecologic Oncology and Cancer Biology, MD Anderson Cancer Center, University of Texas, 1155 Herman Pressler Street, Unit 1362, PO Box 301439, Houston, TX 77230. Phone: 1-713-745-5266; Fax: 1-713-792-7586; E-mail: asood@mdanderson.org

doi: 10.1158/1078-0432.CCR-10-3176

Introduction

In 2010, more than 21,000 women in the United States were diagnosed with ovarian carcinoma and almost 14,000 died from this disease, which ranks as the most common cause of death among gynecologic malignancies (1). The majority of ovarian carcinomas are of serous histology. Mucinous histology is relatively rare, accounting for 2% to 10% of all subtypes of epithelial ovarian carcinomas (2, 3). Because of its relatively rare incidence, mucinous ovarian carcinomas are understudied but are thought to have poorer response to taxane and platinum chemotherapy, resulting in poor survival outcomes compared with serous ovarian carcinomas (4–7). Therefore, understanding the mechanisms contributing to mucinous ovarian cancer development and progression as well as novel therapeutic approaches are urgently needed.

Recent evidence suggests that mucinous ovarian carcinoma is histologically and molecularly similar to colorectal carcinomas and has a distinct clinical pattern compared

Published OnlineFirst July 7, 2011; DOI:10.1158/1078-0432.CCR-10-3176

Translational Relevance

Recent studies have shown that mucinous ovarian carcinomas have a distinct clinical pattern compared with other subtypes of ovarian carcinomas. The first part of our study has shown poorer survival outcome in mucinous ovarian carcinoma than in serous ovarian cancer, the most common subtype of ovarian carcinoma, in a large sample size. Genomic approaches using mucinous ovarian cancer cell lines pointed to the Src kinase being involved in many of the activated pathways. In validation studies, Src was found to be highly activated in mucinous ovarian cancer. The mucinous ovarian cancer cells were resistant to most chemotherapy drugs. An Src inhibitor dasatinib, inhibited oxaliplatin-induced Src activation and enhanced antitumor effects of oxaliplatin in both *in vitro* and *in vivo* models of mucinous ovarian carcinoma. These findings implicate Src as a critical therapeutic target in mucinous ovarian carcinoma.

with other subtypes of ovarian carcinomas (8, 9). The majority of colorectal carcinomas are of mucinous histology, and patients with advanced-stage colorectal carcinoma are treated with chemotherapy containing oxaliplatin, a third-generation platinum compound (10). Despite proven efficacy, resistance to oxaliplatin is a rising issue (11). Among proposed mechanisms, Src kinase has been shown to play an important role in oxaliplatin resistance in colorectal and pancreatic carcinomas (12, 13). Src kinase is a nonreceptor tyrosine kinase that regulates various aspects of tumor progression via multiple signaling pathways, including cell survival (AKT), growth (Ras/MEK/ERK), metastasis (FAK/paxillin/c-Jun), and angiogenesis (STAT3/VEGF; ref. 14). Src kinase is known to be overexpressed in colorectal, pancreatic, lung, breast, and prostate carcinomas (15) and is thought to contribute to chemotherapy resistance (13). In serous ovarian carcinoma, Src kinase was reported to be overexpressed in advanced-stage disease (16). However, the role of Src kinase in mucinous ovarian carcinoma is not known and was examined in this study.

Here, we show that (i) advanced-stage mucinous ovarian carcinoma was associated with shorter survival time after progression or recurrence of disease than with serous histology in a large cohort study, (ii) Src kinase is highly activated among mucinous ovarian carcinomas, and (iii) targeting Src kinase with a combination of oxaliplatin and dasatinib showed synergistic antitumor effects in mucinous ovarian cancer models.

Materials and Methods

Clinical data

A total of 1,302 ovarian cancer patients from cancer centers in the United States and Japan were evaluated; 122 mucinous carcinoma patients (fourth common, 9.4 ± 0.8%) were compared with 698 serous carcinoma patients (most common, 53.4 ± 1.4%) for survival. Patient age, preoperative cancer antigen 125 (CA-125) value, histologic subtypes, International Federation of Gynecology and Obstetrics (FIGO) stage, grade, and cytoreduction were evaluated to determine potential impact on survival. Early- and advanced-stage diseases were defined as FIGO stages I/II and III/IV, respectively. Appendectomy is generally carried out as a standard surgical procedure for mucinous ovarian carcinoma in the participating institutions. Gynecologic pathologists at each institution reviewed all of the specimens for assessing histology. Institutional Review Board approval was obtained at each institution.

Cell lines and cultures

RMUG-S and RMUG-L were cultured in RPMI-1640 media, supplemented with 10% FBS and 0.1% gentamicin at 37°C in 5% CO_2 with 95% air. These cell lines were originally isolated from women with mucinous ovarian carcinoma (17). Ovarian serous carcinoma cell lines (HeyA8, HeyA8-MDR, SKOV3-ip1, and SKOV3-TR), clear cell carcinoma cell lines (ES-2 and RMG-2), and undifferentiated carcinoma cell lines (A2780 and A2780-CP20) were cultured in RPMI-1640 media supplemented with 15% FBS and 0.1% gentamicin at 37°C in 5% CO_2 with 95% air. *In vitro* experiments were conducted with 80% cell confluence. All the cell lines were purchased from American Type Culture Collection or Japanese Collection of Research Bioresources).

Drugs and reagents

Anti-Src (#2108) and anti-phospho-Src (Tyr419; #2101) antibodies for Western blotting were purchased from Cell Signaling Technology. Anti-phospho-Src antibody (Tyr419; AF2685) for immunohistochemical staining was purchased from R&D Systems. Anti-CD31 (#53370) and anti-Ki67 (CP2498) antibodies were purchased from BD Pharmingen and BioCare Medical, respectively. Anti-vinculin (V9131) and anti-β-actin (A5316) antibodies were purchased from Sigma-Aldrich. Oxaliplatin (Wyeth) was purchased from the institutional pharmacy. Dasatinib (Bristol-Myers Squibb) was prepared as a 20 mmol/L stock solution in dimethyl sulfoxide (DMSO). Paclitaxel, cisplatin, carboplatin, doxorubicin, and topotecan were purchased from Sigma-Aldrich. Etoposide was purchased from EMD4 Biosciences.

Microarray analysis

Gene expression was compared between mucinous (RMUG-S and RMUG-L) and serous (SKOV3, OVCA3, 420, 429, 432, and 433) ovarian cancer cell lines. Pathway analysis was used to assess significant genes in mucinous compared with serous ovarian carcinoma (Ingenuity Pathway Analysis, version 7.5; ref. 18; GeneChip Human Genome U133 Plus 2.0 Array). Significant gene network was plotted (both direct and indirect relationship) using the cutoff value of ±1.5-fold change. Src kinase–specific pathway analysis was carried out and was

Published OnlineFirst July 7, 2011; DOI:10.1158/1078-0432.CCR-10-3176

shown as functional gene network ontology. Extraction of networks of molecular interactions for each data set was conducted using NetWalk, a random walk-based network retrieval algorithm (19), and NetWalk-mediated analyses and visualizations were carried out using NetWalker, an integrated platform for network-based data analyses and visualization.

Apoptosis assay

For evaluation of apoptosis, PE Annexin V Apoptosis Detection Kit I (BD Pharmingen) was used as described previously (20). Briefly, 5×10^5 RMUG-S-ip2 cells with serum-containing medium were plated in 10-cm plates and incubated for 24 hours. Then, the media was replaced with fresh serum-free medium. Treatment was started with control, oxaliplatin, dasatinib, and oxaliplatin with dasatinib for time periods ranging from 24 to 96 hours. Cell morphology was assessed by phase-contrast microscopy. Then, cells were removed from plate by trypsin-EDTA, washed twice with PBS, and resuspended with binding buffer at 10^6 cells/mL. FITC Annexin V and propidium iodide were added (each at 5 μL/10^5 cells). Cells were incubated for 15 minutes at room temperature in the dark. Percentage of apoptosis was analyzed with an EPICS XL flow cytometer (Beckman-Coulter). Each sample was analyzed in triplicate.

Cytotoxicity assays

Cytotoxicity of oxaliplatin, dasatinib, and oxaliplatin with dasatinib treatment in RMUG-S-ip2 cells was assessed with MTT uptake assay (Sigma-Aldrich) as described previously (20). Briefly, 2×10^3 RMUG-S-ip2 or SKOV3-TR cells with serum-containing medium were plated in each well of a 96-well plate and incubated for 24 hours. Then, the media was replaced with fresh serum-free medium containing various concentrations of drugs (200 μL). Treatment was stopped at 48-, 72-, and 96-hour time points, and 0.15% MTT (50 μL) was added to each well. After a 2-hour incubation period (37°C), medium was removed from each well and 100 μL of DMSO (Sigma-Aldrich) was added. The absorbance at 570-nm wavelengths was measured by using a Falcon microplate reader (Becton Dickinson Labwave). Each sample was analyzed in triplicate.

Isobologram analysis was carried out to evaluate the cytotoxicity of oxaliplatin and dasatinib in RMUG-S-ip2 based on the dose–response cell survival curves (21). Interaction index was calculated as described previously (22). Additive effect (1), synergistic effect (<1), and antagonistic effect (>1) of the combination of oxaliplatin and dasatinib were determined on the basis of the interaction index.

Cell-cycle analysis

Proportions of cells in G_1, S, and G_2 phases were evaluated following treatment with either oxaliplatin, dasatinib, or oxaliplatin with dasatinib and compared with untreated controls. Briefly, 5×10^5 RMUG-S-ip2 cells with serum-containing medium were plated in a 10-cm dish plate and incubated for 24 hours. Then, the media was replaced with fresh serum-free medium. Treatment in each condition was stopped at 24-, 48-, 72-, and 96-hour time points, and cells were removed from the plate by trypsin-EDTA, washed twice with PBS, and fixed with 70% ethanol (4°C overnight). Ethanol was removed and incubated with propidium iodine for 10 minutes. Cell-cycle analysis was carried out with an EPICS XL flow cytometer (Beckman-Coulter). Each sample was analyzed in triplicate.

Western blotting

Preparation of lysates from cultured cells was carried out as previously described (23, 24). Briefly, cells with 80% confluence were harvested and lysed in modified radioimmunoprecipitation (RIPA) assay buffer (50 mmol/L Tris, 150 mmol/L NaCl, 1% Triton X-100, 0.5% deoxycholate, 25 μg/mL leupeptin, 10 μg/mL aprotinin, 2 mmol/L EDTA, and 1 mmol/L sodium orthovanadate) as described previously (24). Protein concentrations were measured with BCA Protein Assay Reagent Kit (Pierce Biotechnology), and 50 μg of lysate protein was mixed with 10% SDS-PAGE gels transferred electrophoretically onto a nitrocellulose membrane. Nonfat milk powder (5%) in TBS-T [10 mmol/L Tris (pH 8), 150 mmol/L NaCl, and 0.05% Tween-20] was used for protein block for 1 hour. The blots were incubated with anti-Src (band at 60 kDa) and anti-phospho-Src (60 kDa) antibodies at dilutions of 1:1,000 for 4°C overnight and washed with TBS-T. Antibody binding was probed by incubating the blots with horseradish peroxidase–conjugated goat anti-rabbit antibodies (GE Healthcare) in 5% milk diluted with TBS-T for 1 hour at room temperature. Reactivity was visualized with an enhanced chemiluminescence detection kit (Pierce Biotechnology). Anti-vinculin (120 kDa) or anti-β-actin (42 kDa) was used to evaluate an equal protein loading. Densitometry (ImageJ; NIH) was used to interpret the difference in the results of Western blot.

Immunohistochemistry

Immunohistochemical analysis for phospho-Src (Tyr419) and Src kinase was evaluated for human tissue samples embedded in paraffin blocks. For mouse tissues, phospho-Src, Src kinase, and Ki67 were evaluated using formalin-fixed paraffin-embedded tumors. Optimal cutting temperature (OCT) compound-fixed tumor samples were used for CD31 staining. Briefly, the paraffin-embedded block was sectioned to 5-μm thickness and deparaffinized (60°C overnight) and rehydrated. Antigen retrieval was done using the pretreatment reagent Borg Decloaker (BioCare Medical) with pressure cooker for anti-phospho-Src and anti-Src antibodies or Diva (BioCare Medical) with steamer for anti-Ki67 antibody, respectively. For CD31 staining, sections were done on freshly cut frozen slides. These were fixed in cold acetone, and no antigen retrieval was necessary. Endogenous peroxidase and nonspecific epitopes were blocked with 3% H_2O_2 (Fisher Scientific) in PBS for 12 minutes at room temperature, nonspecific protein blinding was blocked with 5% normal

Published OnlineFirst July 7, 2011; DOI:10.1158/1078-0432.CCR-10-3176

horse serum and 1% normal goat serum for anti-Ki67 and anti-CD31 antibodies or 4% cold water fish skin gelatin (Electron Microscopy Science) for anti-phospho-Src or anti-Src antibodies for 20 minutes at room temperature, respectively. Sections were incubated with primary antibodies at 4°C overnight. For negative control, sections were incubated without primary antibody and with human IgG antibody (Jackson ImmunoResearch Laboratories). Goat anti-rabbit horseradish peroxidase–conjugated antibody (Jackson ImmunoResearch Laboratories) for anti-CD31 and anti-Ki67 (1 hour, room temperature) or Mach 4 Universal HRP polymer (BioCare Medical) for anti-phospho-Src and anti-Src antibodies (20 minutes, room temperature) were used for secondary antibody, respectively. Signal was visualized after incubating with 3,3′-diaminobenzidine (Phoenix Biotechnologies) and counterstaining with Gill's no. 3 hematoxylin (Sigma-Aldrich).

Animal care

Nude mice (8–12 weeks old) were purchased from the National Cancer Institute (NCI)/Frederick Cancer Research and Development Center (athymic female, Ncr-nu). The mice were quarantined, housed, and maintained under specific pathogen-free environment in the animal facility that is approved by the American Association for Accreditation of Laboratory Animal Care in agreement with the current regulations and standards of United States Department of Agriculture, Department of Health and Human Service (DHHS), and NIH. Approval of the study protocols was obtained and supervised by the Institutional Animal Care and Use Committee at the University of Texas MD Anderson Cancer Center.

In vivo therapeutic experiment

In vivo model of mucinous ovarian carcinoma (RMUG-S-ip2) was created for the experiment (Supplementary Methods) and the characteristics are shown in Supplementary Figure S1. RMUG-S-ip2 cells were injected into the peritoneal cavity of 40 orthotopic nude mice (4×10^6 cells/mouse). After randomization into 4 groups of 10 mice (control, oxaliplatin alone, dasatinib alone, and oxaliplatin with dasatinib), treatment was initiated at 4 weeks following injection. Oxaliplatin (5 mg/kg/mouse) was given intraperitoneally (i.p.) twice weekly after being dissolved in 5% dextrose and diluted with HBSS (13). Dasatinib (15 mg/kg/d/mouse) was given orally every day after being solubilized in citrate/citric acid buffer. Control mice received HBSS i.p. twice a week and citrate buffer orally every day. Mice were monitored on a daily basis and weighted weekly. After 8 weeks of treatment, the mice were sacrificed and total body weight of mouse, tumor locations and weight, and the number of tumor nodules were recorded. Tumor samples were fixed with 10% formalin and embedded in paraffin or with OCT compound in liquid nitrogen. A similar experiment was conducted with 25% drug dose reduction for both oxaliplatin and dasatinib in the RMUG-S-ip2 model. In addition, an experiment with the SKOV3-TR model (1.25×10^6 cells/mouse) was carried out (mice were randomized into 4 groups as noted earlier and treatment was started 1 week after tumor cell injection and continued for 5 weeks).

Statistical analysis

Continuous variables were assessed for normal distribution (Kolmogorov–Smirnov test) and expressed as appropriate (mean ± SD (or SE) or median with range). Student's *t* test or the Mann–Whitney *U* test was conducted to determine the statistical significance. Categorical variables were evaluated with Fisher's exact test (OR and 95% CI). For clinical data analysis, to determine the significance of variables for the survival outcomes, such as progression-free survival (PFS), overall survival (OS), and survival time after progression of disease or recurrence, univariate (log-rank test) and multivariate (Cox regression proportional hazard test) analyses were carried out as appropriate. Survival curves were estimated with the Kaplan–Meier method. *P* values of less than 0.05 were considered as statistically significant (all, 2-tailed). The Statistical Package for Social Scientists software (SPSS; version 18.0) was used for all analyses.

Results

Mucinous ovarian carcinomas have distinct clinical characteristics

We first examined the clinical features of mucinous ovarian carcinoma compared with serous subtypes. The average age of women with a diagnosis of mucinous carcinoma was significantly less than those with serous carcinoma (mean age, 54.1 ± 14.8 vs. 59.9 ± 11.3, $P = 0.005$). Distribution of FIGO stages among women with mucinous carcinomas was also significantly different from those with serous histology; majority of mucinous cases were early-stage carcinomas, whereas majority of serous cases were advanced-stage carcinomas ($P < 0.0001$; Fig. 1A). CA-125 is a common biomarker for ovarian cancer used for diagnosis or follow-up after therapy. In women with mucinous ovarian carcinomas, CA-125 was infrequently elevated compared with those with serous carcinoma (proportion of elevated CA-125 >35 IU/L in all stage cases, 66.7% vs. 96.0%, OR 0.56, 95% CI 0.38–0.83, $P < 0.0001$; Fig. 1B). Same results were noted in advanced-stage carcinomas (78.6% vs. 97.4%, OR 0.1, 95% CI 0.02–0.43, $P = 0.009$). Among cases with elevated CA-125 (>35 IU/L), mucinous carcinoma patients showed lower CA-125 values than those with serous carcinoma (median 229 vs. 475 IU/L, $P < 0.0001$; Fig. 1B). In multivariate analysis adjusted for other significant variables, such as age, cytoreduction, and stage, mucinous histology remained an independent risk factor for survival of ovarian cancer patients (OS, $P = 0.045$; survival time after recurrence, $P < 0.0001$). In early-stage disease, mucinous carcinoma patients showed better survival outcomes than those with serous carcinoma (10-year PFS, 78.7% vs. 66.6%, $P = 0.039$; 10-year OS, 89.5% vs. 53.6%, $P = 0.086$; Fig. 1C). This difference likely represents the lower frequency of recurrence in women with

Published OnlineFirst July 7, 2011; DOI:10.1158/1078-0432.CCR-10-3176

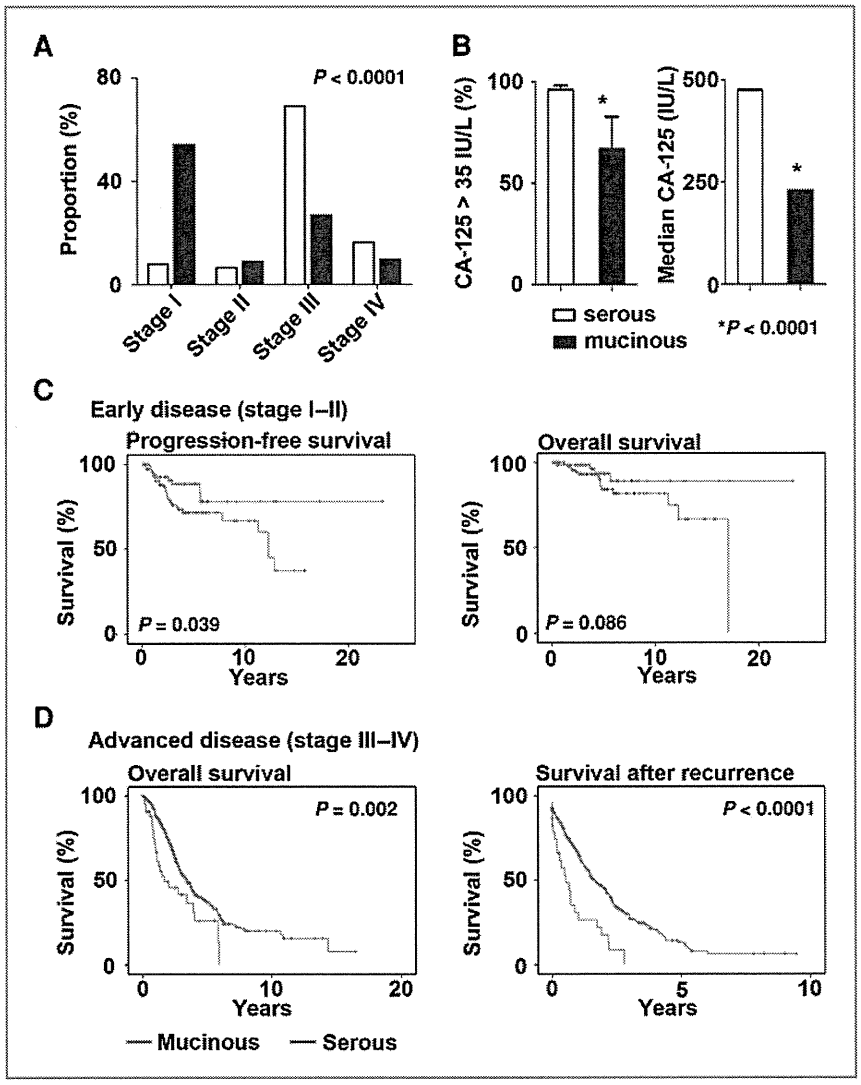

Figure 1. Clinical significance of mucinous ovarian carcinomas. A, the proportion of FIGO stage in 122 mucinous (black bar) and 698 serous (white bar) carcinoma patients is shown. B, the proportion of patients with elevated CA-125 (>35 IU/L) and median CA-125 value among patients with mucinous or serous carcinomas is shown. Bar for CA-125, more than 35 IU/L represents frequency with 95% CI. C, Kaplan–Meier survival curves for PFS and OS in early-stage disease are shown. D, Kaplan–Meier survival curves for OS and survival time after progression or recurrence of disease are shown.

early-stage mucinous ovarian carcinoma than among those with serous histology (12.5% vs. 30%, OR 0.33, 95% CI 0.15–0.76, $P = 0.009$). In advanced-stage disease, representing 36.9% of mucinous ovarian carcinoma cases, although there was no statistically significant difference in PFS between mucinous and serous carcinoma patients ($P = 0.92$), OS of mucinous carcinoma patients was significantly shorter than those with serous carcinoma (median OS, 1.67 vs. 3.41 years, $P = 0.002$, multivariate analysis). Similarly, survival time after progression of disease or recurrence after primary cytoreductive surgery was significantly shorter for women with mucinous carcinoma than for those with serous histology (median survival time, 0.53 vs. 1.66 years, $P < 0.0001$, multivariate analysis).

Gene expression and protein activity of Src kinase in mucinous ovarian carcinomas

Given the poor clinical outcome of women with mucinous ovarian cancer, new therapeutic approaches are needed. In search of potentially useful targets, we next evaluated gene expression in mucinous ovarian cancer cell lines (heat map shown in Supplementary Fig. S2). In pathway analysis, 41,329 genes were identified and 12,568 genes were functional and eligible for analysis. The top 5 functional networks and 10 significant genes in mucinous ovarian carcinomas, when compared with serous ovarian carcinomas, are shown in Supplementary Table S1 and Figure S3A–E, respectively. Src kinase was included in the top 3 networks for amino acid, molecular transport, and small molecular biochemistry, although Src

Published OnlineFirst July 7, 2011; DOI:10.1158/1078-0432.CCR-10-3176

mRNA was not differentially expressed between mucinous and serous cancer cell lines (Supplementary Fig. S3C). These data suggest that regulation of Src would be at the protein level. Thus, we examined the phosphorylation status of Src in 12 ovarian cancer lines and 10 clinical mucinous ovarian cancer samples. Because Src kinase activity is proposed to be an important mechanism of resistance to chemotherapy (13), Src kinase–specific pathway analysis was carried out for mucinous compared with serous ovarian carcinoma cell lines (Fig. 2A). Among upregulated genes associated with Src kinase, 3 of 12 genes were cadherin and catenin family members (*CDH1*, *CDH5*, and *JUP*; Supplementary Table S2). Because increased expression of E-cadherin is a characteristic molecular feature of mucinous ovarian carcinoma (25), the increased activity of cadherin/catenin pathway in mucinous ovarian carcinoma may be associated with decreased Src expression in mucinous ovarian carcinoma. There were some downregulated genes associated with cell growth, adhesion, and motility in the mucinous ovarian cancer cells (*ASAP1*, *ITGB3*, *RAC2*, *DNM1*, and *MYLK*; Supplementary Table S2).

Next, protein expression of Src kinase was evaluated in 12 ovarian cancer cell lines and 2 nontransformed cell lines. The results were similar to the microarray analysis, and the level of total Src expression in mucinous ovarian carcinoma cell line (RMUG-S-ip2) was the lowest among tested cell lines (Fig. 2B). However, RMUG-S-ip2 showed the highest activity of Src kinase, as determined by the ratio between phospho-Src kinase and Src kinase. Expression of Src kinase [total Src and phospho-Src (Tyr419)] was also evaluated in 10 mucinous ovarian cancer samples (Fig. 2C). p-SrcY419 was localized in the cytoplasm of cancer cells, and all samples showed overexpression of Src kinase.

Mucinous ovarian carcinomas are drug resistant

On the basis of clinical findings suggesting relative drug resistance, we next examined the sensitivity of mucinous (RMUG-S and RMUG-L) and serous (SKOV3) ovarian cancer cell lines to various chemotherapeutic agents (Fig. 2D). Compared with serous cancer cell line, mucinous carcinoma cell lines had significantly higher IC_{50} values for all tested chemotherapeutic agents. IC_{50} doses for oxaliplatin in RMUG-S-ip2 and RMUG-L-ip2 cells were 15.6 and 16.4 μg/mL, respectively (Supplementary Fig. S4). These values are comparable with colorectal cancer cell lines reported previously (2.8–29 μg/mL; refs. 26, 27). IC_{50} level of oxaliplatin in drug resistant–cell line SKOV3-TR cells was 5.2 μg/mL (Supplementary Fig. S4).

Oxaliplatin-induced Src kinase activity is inhibited by dasatinib

Next, we examined the effects of oxaliplatin on Src expression and activation in the RMUG-S-ip2 and SKOV3-TR cells. Oxaliplatin induced Src phosphorylation but had no effect on total Src levels in the RMUG-S-ip2 cells (Fig. 3A). Oxaliplatin did not affect Src phosphorylation in the SKOV3-TR cells (Supplementary Fig. S5). Treatment with dasatinib downregulated the phosphorylation of Src kinase in the RMUG-S-ip2 cells (Fig. 3B). We then examined the effect of the combination of oxaliplatin and dasatinib on Src activation in RMUG-S-ip2 cells. In combination treatment, dasatinib blocked the oxaliplatin-induced increase in Src activity (Fig. 3B).

We next examined the effect of dasatinib on cell viability in the RMUG-S-ip2 and SKOV3-TR cells. RMUG-S-ip2 cells showed a dose-dependent decrease in cell viability with dasatinib (Fig. 4A). Conversely, SKOV3-TR cells did not show changes in viability with dasatinib (Fig. 4B). RMUG-S-ip2 cells were then treated with various concentrations of oxaliplatin and dasatinib (Fig. 4C). Oxaliplatin treatment alone affected cell viability of RMUG-S-ip2 cells (IC_{50}, 15.6 μg/mL), and the addition of dasatinib enhanced cytotoxic effects of oxaliplatin treatment. Isobologram analysis was carried out, and the interaction index was less than 1 at all examined points, confirming the synergistic effects of oxaliplatin and dasatinib in cell viability (Fig. 4D). Dasatinib concentration of 182 nmol/L showed a 50% reduction of oxaliplatin IC_{50}. In the SKOV3-TR cells, there was no difference in cell viability between oxaliplatin treatment alone and oxaliplatin with dasatinib (data not shown).

Effects of combination therapy with oxaliplatin and dasatinib were evaluated using apoptosis assays in RMUG-S-ip2 cells (Fig. 4E and Supplementary Fig. S6A). Monotherapy with either oxaliplatin or dasatinib significantly increased apoptosis compared with controls (proportion of apoptosis, control vs. dasatinib vs. oxaliplatin, 4.1 ± 0.8 vs. 8.5 ± 0.3 vs. $9.5 \pm 0.5\%$; for both oxaliplatin and dasatinib, $P < 0.01$). Combination therapy with oxaliplatin and dasatinib further enhanced the extent of apoptosis compared with monotherapy either with dasatinib or with oxaliplatin (proportion of apoptosis, combination therapy vs. dasatinib vs. oxaliplatin, 26.8 ± 0.3 vs. 8.5 ± 0.3 vs. $9.5 \pm 0.5\%$; for both oxaliplatin and dasatinib, $P < 0.01$). These significant effects were observed at all time points examined (24–96 hours), and the effects were maximal at the 96-hour time point. Effects of therapy on cell-cycle were also analyzed in the RMUG-S-ip2 cells (Fig. 4F and Supplementary Fig. S6B). Oxaliplatin significantly increased the proportion of cells in S-phase and decreased in both G_1 and G_2 phases compared with control ($P < 0.001$). Dasatinib treatment did not affect cell-cycle distribution. The results of the combination of oxaliplatin and dasatinib remained similar to the results of oxaliplatin treatment ($P < 0.001$ compared with control).

In vivo antitumor effects of oxaliplatin and dasatinib in ovarian carcinoma

Next, an *in vivo* experiment was carried out to evaluate the antitumor effects of combination therapy with oxaliplatin and dasatinib. Compared with the control group, monotherapy with oxaliplatin or dasatinib resulted in significantly smaller tumor weight (tumor weight reduction, control vs. oxaliplatin, 58.6%, $P < 0.01$; and control vs. dasatinib 65.8%, $P < 0.01$) and number of tumor

Published OnlineFirst July 7, 2011; DOI:10.1158/1078-0432.CCR-10-3176

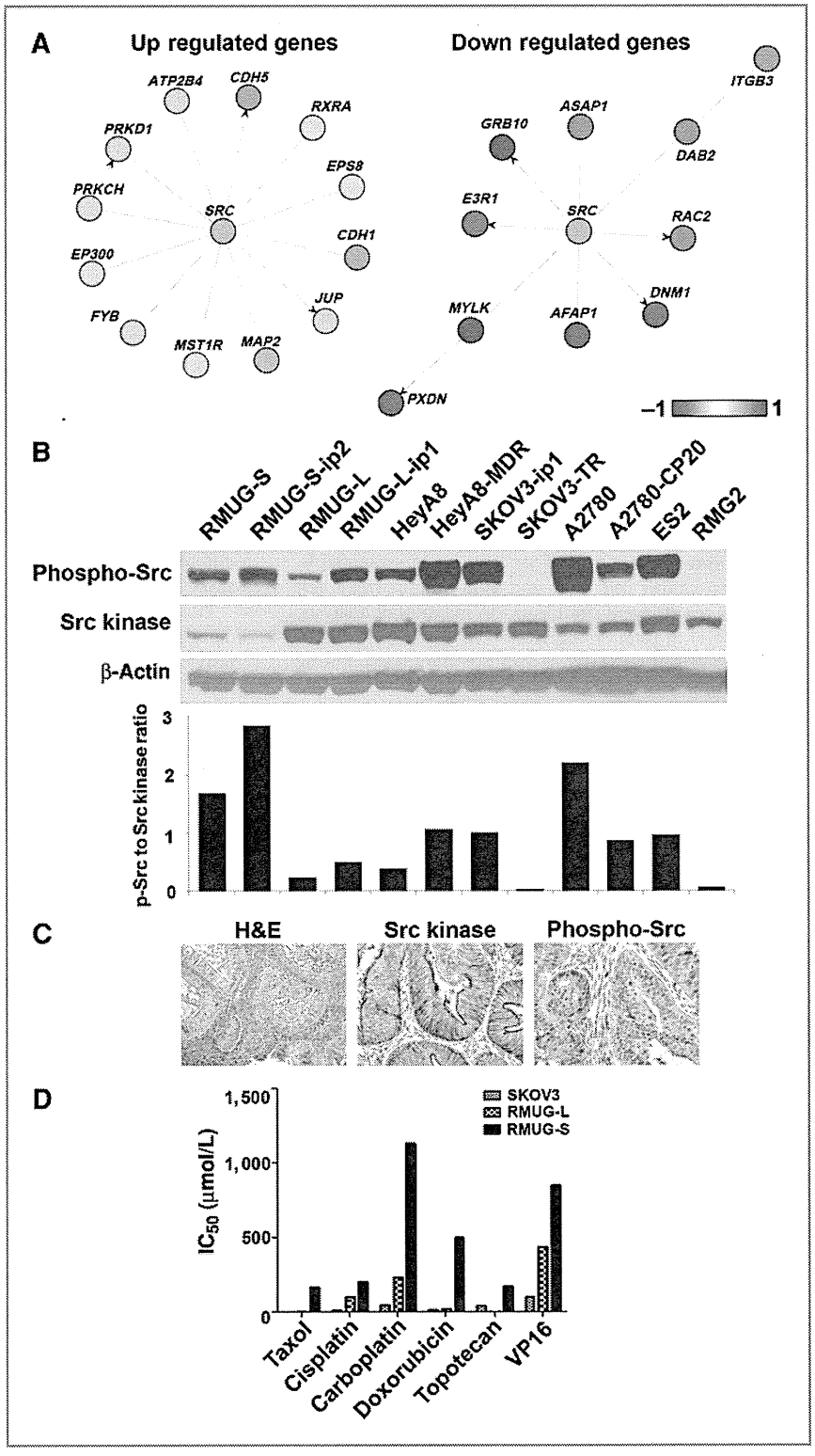

Figure 2. Expression and activity of Src kinase in mucinous ovarian carcinomas. A, Src pathway–specific analysis with gene network ontology is shown. Expression in mucinous ovarian carcinoma cell lines was compared with serous ovarian carcinoma cell lines. B, Western blot analysis for phospho-Src and Src kinase in 14 cell lines is shown. C, immunohistochemical staining for Src kinase and phospho-Src in human mucinous ovarian carcinomas is shown (magnification 200×). H&E, hematoxylin–eosin. D, cell viability assay for 3 cell lines and 6 chemotherapeutic agents is shown.

Published OnlineFirst July 7, 2011; DOI:10.1158/1078-0432.CCR-10-3176

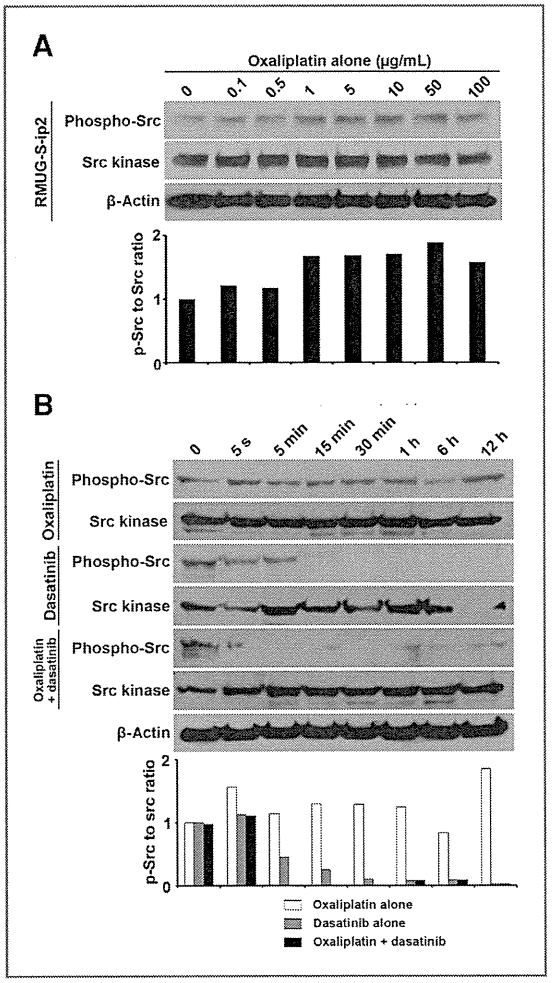

Figure 3. Modulation of Src kinase activity with oxaliplatin and dasatinib. A, Western blot analysis for phospho-Src and Src is shown over various oxaliplatin doses in RMUG-S-ip2 cells after treatment for 30 minutes. B, Western blot analysis for phospho-Src and Src over time is shown for RMUG-S-ip2 cells treated with oxaliplatin (12.4 μg/mL), dasatinib (100 nmol/L), and the combination of the 2 drugs.

nodules (tumor nodule reduction, control vs. oxaliplatin, 45.9%, $P < 0.05$; and control vs. dasatinib 53.6%, $P < 0.05$; Fig. 5A). Combination therapy with oxaliplatin and dasatinib further showed significant antitumor effects compared with either monotherapy: reduction of tumor weight, oxaliplatin versus combination, 79.1%, $P < 0.01$; and dasatinib versus combination, 74.7%, $P < 0.01$, respectively (Fig. 5A). Compared with controls, combination therapy resulted in 91.3% tumor weight reduction and 77.4% decrease in tumor nodule number, respectively (both $P < 0.01$). There were 4 of 10 mice with metastasis to liver parenchyma in the control group, but none in the treatment groups. Mice treated with dasatinib did not have any differences in body weight compared with the control group (data not shown). To evaluate whether there may be synergistic antitumor activity with oxaliplatin and dasatinib, we conducted an *in vivo* experiment using RMUG-S-ip2 with 25% dose reduction of oxaliplatin and dasatinib (Supplementary Fig. S7). The results of antitumor effects in low-dose oxaliplatin and dasatinib were similar to the results of original experiment: antitumor effects of oxaliplatin alone, dasatinib alone, and combination of oxaliplatin and dasatinib were 65.4%, 60.3%, and 88.8%, respectively, when compared with the control group (all $P < 0.05$). These results suggest possible synergistic antitumor effects of oxaliplatin and dasatinib in mucinous ovarian carcinoma.

In contrast to mucinous ovarian carcinoma, serous ovarian carcinoma showed different antitumor effects with dasatinib treatment (Fig. 5A). Although RMUG-S-ip2 showed significant antitumor effects with dasatinib monotherapy, there were no significant antitumor effects in the SKOV3-TR model (mean tumor weight, dasatinib vs. control, 1.09 ± 0.29 vs. 1.42 ± 0.29, $P = 0.42$). These *in vivo* effects with dasatinib monotherapy corresponded well with the effects noted in the *in vitro* experiments with the mucinous and serous cancer cell lines (Fig. 4A and B). Oxaliplatin alone showed significant antitumor effects in the SKOV3-TR model when compared with control (mean tumor weight, oxaliplatin vs. control, 0.48 ± 0.12 vs. 1.42 ± 0.29, $P = 0.01$), and the extent of tumor reduction rate with oxaliplatin therapy was similar to the RUMG-S-ip2 model (58.6% and 65.9%, respectively).

Immunohistochemical staining was carried out on the RMUG-S-ip2 tumor tissues obtained from the *in vivo* experiments to assess the effects on proliferation and microvessel density (MVD; Fig. 5B). Tumors obtained from the dasatinib treatment group showed substantially decreased p-SrcY419 expression compared with the control group. In tumors obtained from the oxaliplatin treatment group, there were areas that showed focally increased expression of p-SrcY419. This was not seen in tumors treated with oxaliplatin and dasatinib. This induction of activated Src following oxaliplatin treatment supports the *in vitro* findings. Numbers of positive-Ki67 cells as well as MVD were significantly decreased in the combination therapy group compared with monotherapy group (all $P < 0.05$; Fig. 5B).

Discussion

Our clinical, *in vitro*, and *in vivo* results highlight important features that contribute to the distinct mechanisms of mucinous ovarian carcinoma pathogenesis. Targeting Src kinase with dasatinib inhibited oxaliplatin-induced Src kinase activity and showed synergistic antitumor effects in a mucinous ovarian carcinoma model. Several key areas in this notable observation deserve special mention.

Mucinous ovarian carcinoma is known to be associated with poorer patient outcome than with other subtypes of ovarian carcinoma (4, 7, 8). Our results not only support previous studies but also imply that mucinous ovarian

Published OnlineFirst July 7, 2011; DOI:10.1158/1078-0432.CCR-10-3176

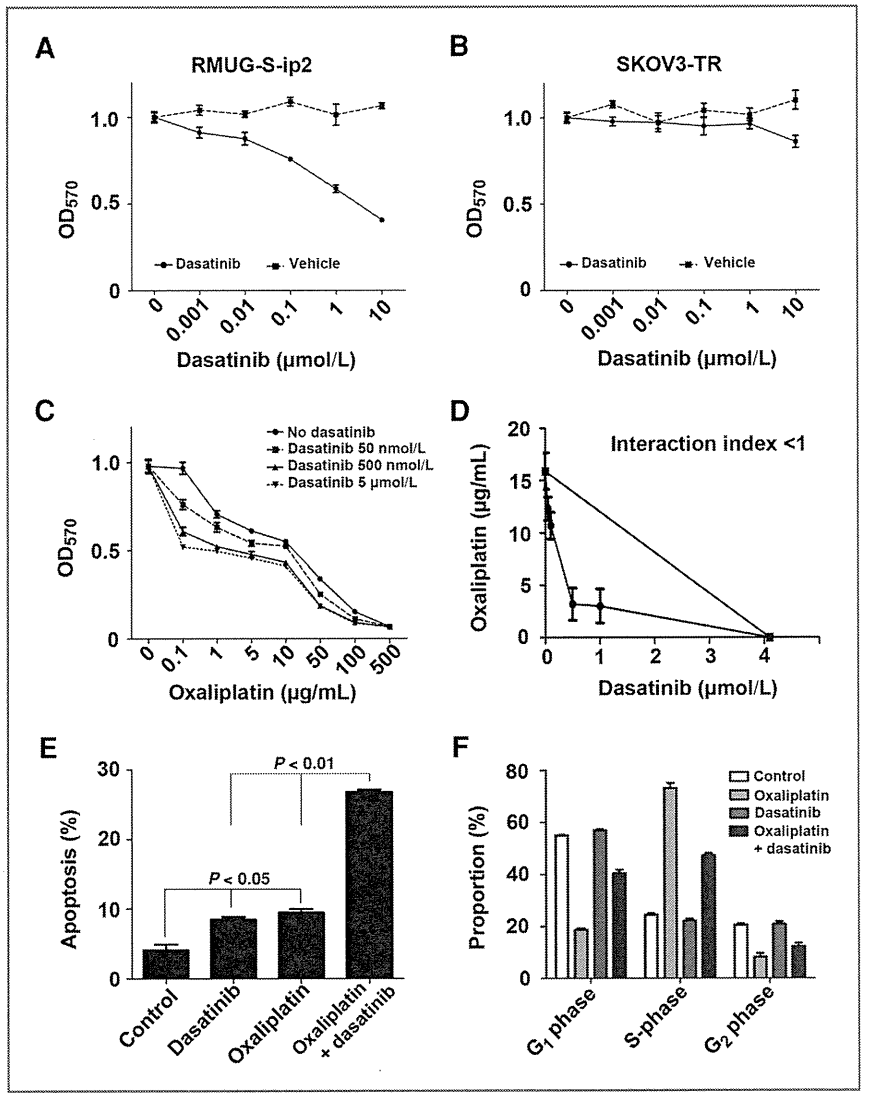

Figure 4. *In vitro* effects of combination therapy with oxaliplatin and dasatinib in mucinous ovarian carcinoma. A and B, cell viability assays for dasatinib treatment in RMUG-S-ip2 (A) and SKOV3-TR (B) cells are shown. IC_{50} dose of dasatinib in RMUG-S-ip2 was 3.1 μmol/L. DMSO was used as the drug vehicle. C, cell viability assay for the combination of oxaliplatin and dasatinib in RMUG-S-ip2 cells is shown following treatment for 72 hours. D, isobologram analysis for oxaliplatin and dasatinib in RMUG-S-ip2 cells is shown. Interaction index was less than 1 at all examined points. Dasatinib concentration that reduced 50% of oxaliplatin IC_{50} dose was 182 nmol/L. E, apoptosis assays for oxaliplatin and dasatinib are shown at the 96-hour time point. Chemotherapeutic doses used for the assay were oxaliplatin 12.4 μg/mL and dasatinib 100 nmol/L, respectively. F, cell-cycle analysis of RMUG-S-ip2 cells treated with oxaliplatin and dasatinib is shown. A–D, dots represent mean ± SE. E and F, bars represent mean ± SE.

carcinomas are associated with slow progression and chemoresistance that may partly be explained by the hypothesis that mucinous ovarian carcinomas are genetically stable (28). To explain the distinct clinical characteristics of mucinous ovarian carcinomas, there are several molecular characteristics that can distinguish these tumors from serous carcinomas (8). Well-studied biomarkers of mucinous ovarian carcinomas include cadherin, matrix metalloproteinases, WT-1, CA-125, and carcinoembryonic antigen. In gene expression analyses with microarrays, the profile patterns among these 2 cell lines were distinctly different (8). Although mucinous ovarian carcinomas are less likely to have *BRCA* or *p53* mutations, *Kras* mutations are seen with greater frequency than with serous carcinomas (8). *Kras* mutation, reported in nearly 40% of carcinomas, is also common in colorectal carcinoma (29). These molecular characteristics further support the premise that mucinous ovarian carcinoma is distinct not only from serous ovarian carcinomas but also from histologically and molecularly mimics colorectal carcinoma (8).

Oxaliplatin has been used for the treatment of ovarian carcinomas in various clinical trials and has shown a wide range of antitumor activity (20%–75%; refs. 12, 30). Induction of Src kinase activity via reactive oxygen species (ROS) produced during the process of oxaliplatin–DNA adduct formation has been proposed as one of the mechanisms associated with oxaliplatin resistance in colorectal carcinoma (13). Thus, dasatinib holds potential

Published OnlineFirst July 7, 2011; DOI:10.1158/1078-0432.CCR-10-3176

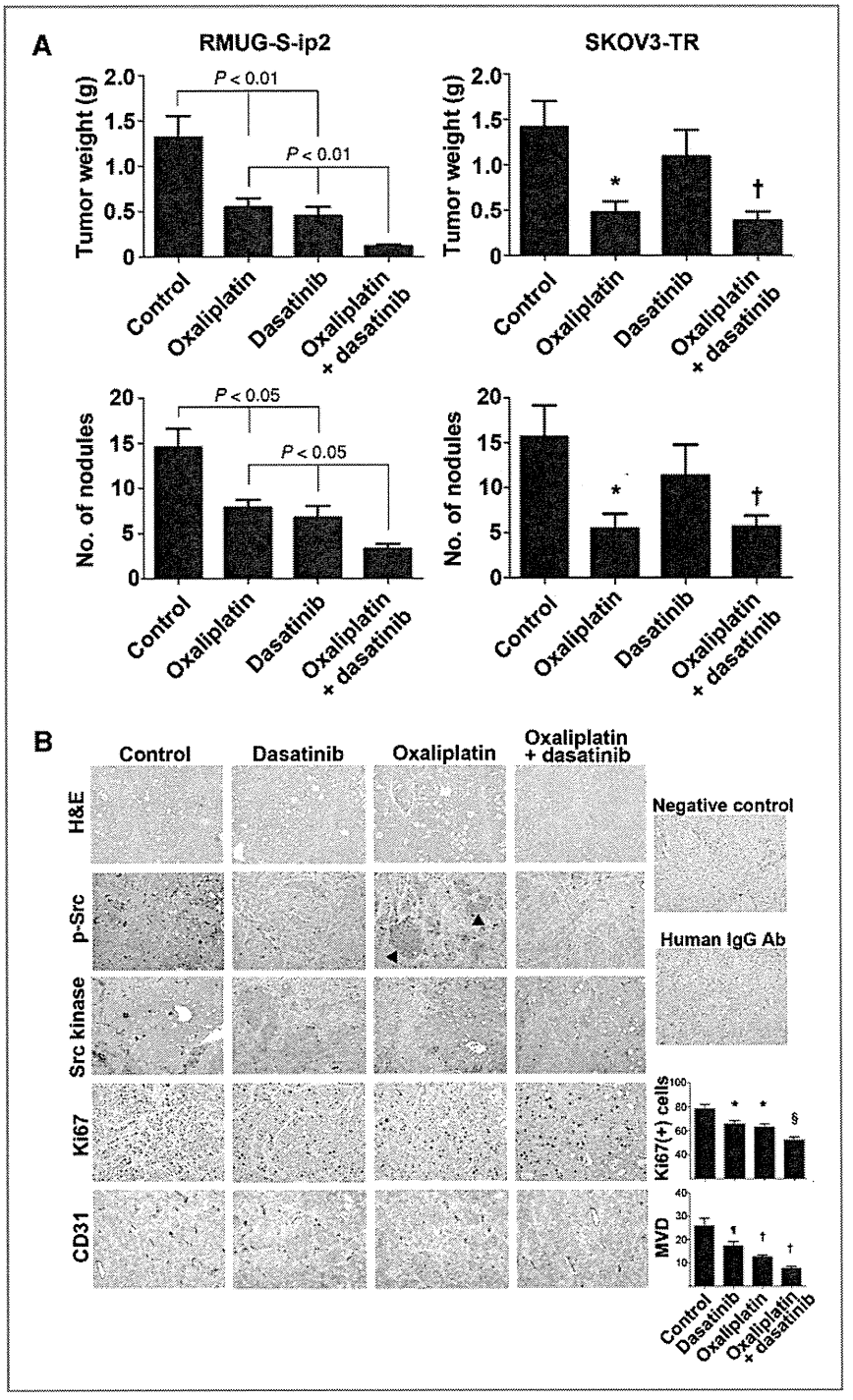

Figure 5. *In vivo* effects of combination therapy with oxaliplatin and dasatinib in ovarian carcinoma. A, tumor weight (top half) and number of nodules (bottom half) are shown for the RMUG-S-ip2 (right) and SKOV3-TR (left) models. Treatment was started 4 weeks from RMUG-S-ip2 cell injection and continued for 8 weeks. For the SKOV3-TR model, treatment was started 1 week after cell injection and continued for 5 weeks. Bar represents mean ± SE. *, $P = 0.01$ (vs. control group). B, immunohistochemical staining for phospho-Src (p-Src), Src kinase, Ki67, and CD31 is shown in 4 groups. For negative control, (i) no primary antibody and (ii) human IgG antibody (Ab) were used. Arrowhead, focally increased expression of p-Src in tumors treated with oxaliplatin. For Ki67 staining, *, $P < 0.01$; §, $P < 0.0001$, compared with control (number of positive Ki67 cells per 100× field). For CD31 staining, ¶, $P < 0.05$; †, $P < 0.01$, compared with control. MVD, number of microvessel per 200× field; H&E, hematoxylin–eosin.

for enhancing the efficacy of oxaliplatin chemotherapy (31). In our study, similar findings were observed in mucinous ovarian carcinoma and treatment with oxaliplatin induced activation of Src kinase in RMUG-S-ip2 cells. Similar induction was not observed in serous ovarian cancer cells. Induction of Src kinase activity may be

Published OnlineFirst July 7, 2011; DOI:10.1158/1078-0432.CCR-10-3176

associated with drug resistance via AKT and Ras pathways in mucinous ovarian carcinoma (13, 32, 33). However, it is not completely clear how Src kinase activity is induced in mucinous ovarian carcinoma but not in serous cancer cells. To date, the mechanism of ROS-induced Src activation is not fully understood (13). As shown in colorectal carcinoma models, pretreatment with an antioxidant agent, such as a vitamin E analogue, inhibited phosphorylation of Src kinase (13). Thus, it is possible that cell innate functions of antioxidative enzymes such as superoxide dismutase in mucinous ovarian carcinoma may be different from that of serous carcinoma (13).

Mucinous ovarian carcinomas showed not only induction of Src kinase activity with oxaliplatin treatment but also increased activity of Src kinase in nonstress conditions. However, expression of Src kinase at mRNA and protein levels in RMUG-S-ip2 cells was lower than in serous cancer cell lines. This suggests that there is a mechanism that contributes to the activation of Src kinase at the protein level but not necessarily at the gene expression level. Theoretically, increased upstream signaling, phosphatase activity, and protein–protein interactions downstream of Src could be the mechanisms that explain increased activity of Src kinase. To date, there is little evidence about the mutation of Src kinase (14, 15). Phosphorylation of Y419 tyrosine residue activates Src kinase, whereas that of Y530 tyrosine residue inactivates Src kinase (15). It is possible that the RMUG-S-ip2 cells may have increased phosphatase activity that dephosphorylates Y530. For protein–protein interaction as the mechanism of Src kinase activation, there are several binding partners of Src kinase that can regulate its catalytic activity including the p130cas/paxillin complex (34). Role of p130cas/paxillin in mucinous ovarian carcinomas is yet to be elucidated and needs further investigation. Because RMUG-S-ip2 cells showed highest Src activity whereas SKOV3-TR showed minimum Src activity, baseline activity of Src kinase may be a predictor of response to dasatinib therapy.

In summary, mucinous ovarian carcinoma has distinct characteristics from serous carcinoma. In light of results presented here, combination therapy with oxaliplatin and dasatinib is an attractive approach for further clinical development.

Disclosure of Potential Conflicts of Interest

No potential conflicts of interest were disclosed.

Acknowledgments

The authors thank Donna Reynolds and Dr. Robert Langley for their technical expertise and helpful discussion.

Grant Support

Portions of this work were supported by the NIH (grants CA110793, 109298, P50 CA083639, P50 CA098258, CA128797, and RC2GM092599), the Ovarian Cancer Research Fund, Inc. (Program Project Development Grant), the DOD (grants OC073399, OC093146, BC085265), the Zarrow Foundation, the Marcus Foundation, the Betty Anne Asche Murray Distinguished Professorship, NCI Institutional Core Grant CA16672, NCI-DHHS-NIH T32 Training Grant (T32 CA101642), GCF/Gail MacNeil KOH Research Grant, Meyer and Ida Gordon Foundation #2 and GCF/OCRF Ann Schreiber Ovarian Cancer Research Grant.

The costs of publication of this article were defrayed in part by the payment of page charges. This article must therefore be hereby marked *advertisement* in accordance with 18 U.S.C. Section 1734 solely to indicate this fact.

Received December 2, 2010; revised June 15, 2011; accepted June 15, 2011; published OnlineFirst July 7, 2011.

References

1. Jemal A, Siegel R, Xu J, Ward E. Cancer statistics, 2010. CA Cancer J Clin 2010;60:277–300.
2. Harrison ML, Jameson C, Gore ME. Mucinous ovarian cancer. Int J Gynecol Cancer 2008;18:209–14.
3. Matsuo K, Bond VK, Eno ML, Im DD, Rosenshein NB. Low drug resistance to both platinum and taxane chemotherapy on an *in vitro* drug resistance assay predicts improved survival in patients with advanced epithelial ovarian, fallopian and peritoneal cancer. Int J Cancer 2009;125:2721–7.
4. Hess V, A'Hern R, Nasiri N, King DM, Blake PR, Barton DP, et al. Mucinous epithelial ovarian cancer: a separate entity requiring specific treatment. J Clin Oncol 2004;22:1040–4.
5. Winter WE 3rd, Maxwell GL, Tian C, Carlson JW, Ozols RF, Rose PG, et al. Prognostic factors for stage III epithelial ovarian cancer: a Gynecologic Oncology Group study. J Clin Oncol 2007;25: 3621–7.
6. Bamias A, Psaltopoulou T, Sotiropoulou M, Haidopoulos D, Lianos E, Bournakis E, et al. , Mucinous but not clear cell histology is associated with inferior survival in patients with advanced stage ovarian carcinoma treated with platinum-paclitaxel chemotherapy. Cancer 2010; 116:1462–8.
7. Shimada M, Kigawa J, Ohishi Y, Yasuda M, Suzuki M, Hiura M, et al. Clinicopathological characteristics of mucinous adenocarcinoma of the ovary. Gynecol Oncol 2009;113:331–4.
8. Frumovitz M, Schmeler KM, Malpica A, Sood AK, Gershenson DM. Unmasking the complexities of mucinous ovarian carcinoma. Gynecol Oncol 2010;117:491–6.
9. Gomez-Raposo C, Mendiola M, Barriuso J, Hardisson D, Redondo A. Molecular characterization of ovarian cancer by gene-expression profiling. Gynecol Oncol 2010;118:88–92.
10. Cunningham D, Atkin W, Lenz HJ, Lynch HT, Minsky B, Nordlinger B, et al. Colorectal cancer. Lancet 2010;375:1030–47.
11. Almendro V, Ametller E, Garcia-Recio S, Collazo O, Casas I, Augé JM, et al. The role of MMP7 and its cross-talk with the FAS/FASL system during the acquisition of chemoresistance to oxaliplatin. PLoS One 2009;4:e4728.
12. Fu S, Kavanagh JJ, Hu W, Bast RC Jr. Clinical application of oxaliplatin in epithelial ovarian cancer. Int J Gynecol Cancer 2006;16: 1717–32.
13. Kopetz S, Lesslie DP, Dallas NA, Park SI, Johnson M, Parikh NU, et al. Synergistic activity of the SRC family kinase inhibitor dasatinib and oxaliplatin in colon carcinoma cells is mediated by oxidative stress. Cancer Res 2009;69:3842–9.
14. Summy JM, Gallick GE. Treatment for advanced tumors: SRC reclaims center stage. Clin Cancer Res 2006;12:1398–401.
15. Kim LC, Song L, Haura EB. Src kinases as therapeutic targets for cancer. Nat Rev Clin Oncol 2009;6:587–95.
16. Wiener JR, Windham TC, Estrella VC, Parikh NU, Thall PF, Deavers MT, et al. Activated SRC protein tyrosine kinase is overexpressed in late-stage human ovarian cancers. Gynecol Oncol 2003;88:73–9.
17. Sakayori M, Nozawa S, Udagawa Y, Chin K, Lee SG, Sakuma T, et al. [Biological properties of two newly established cell lines (RMUG-S, RMUG-L) from a human ovarian mucinous cystadenocarcinoma]. Hum Cell 1990;3:52–6.

Published OnlineFirst July 7, 2011; DOI:10.1158/1078-0432.CCR-10-3176

18. Helleman J, Smid M, Jansen MP, van der Burg ME, Berns EM. Pathway analysis of gene lists associated with platinum-based chemotherapy resistance in ovarian cancer: the big picture. Gynecol Oncol 2010;117:170–6.
19. Komurov K, Padron D, Cheng T, Roth M, Rosenblatt KP, White MA. Comprehensive mapping of the human kinome to epidermal growth factor receptor signaling. J Biol Chem 2010;285: 21134–42.
20. Lee JW, Han HD, Shahzad MM, Kim SW, Mangala LS, Nick AM, et al. EphA2 immunoconjugate as molecularly targeted chemotherapy for ovarian carcinoma. J Natl Cancer Inst 2009;101: 1193–205.
21. Machado SG, Robinson GA. A direct, general approach based on isobolograms for assessing the joint action of drugs in pre-clinical experiments. Stat Med 1994;13:2289–309.
22. Lu G, Xiao H, You H, Lin Y, Jin H, Snagaski B, et al. Synergistic inhibition of lung tumorigenesis by a combination of green tea polyphenols and atorvastatin. Clin Cancer Res 2008;14: 4981–8.
23. Halder J, Kamat AA, Landen CN Jr, Han LY, Lutgendorf SK, Lin YG, et al. Focal adhesion kinase targeting using *in vivo* short interfering RNA delivery in neutral liposomes for ovarian carcinoma therapy. Clin Cancer Res 2006;12:4916–24.
24. Mangala LS, Zuzel V, Schmandt R, Leshane ES, Halder JB, Armaiz-Pena GN, et al. Therapeutic targeting of ATP7B in ovarian carcinoma. Clin Cancer Res 2009;15:3770–80.
25. Sarrio D, Moreno-Bueno G, Sanchez-Estevez C, Banon-Rodriguez I, Hernandez-Cortes G, Hardisson D, et al. Expression of cadherins and catenins correlates with distinct histologic types of ovarian carcinomas. Hum Pathol 2006;37:1042–9.
26. Flis S, Splwinski J. Inhibitory effects of 5-fluorouracil and oxaliplatin on human colorectal cancer cell survival are synergistically enhanced by sulindac sulfide. Anticancer Res 2009;29:435–41.
27. Jiang H, Chen K, He J, Pan F, Li J, Chen J, et al. Association of pregnane X receptor with multidrug resistance-related protein 3 and its role in human colon cancer chemoresistance. J Gastrointest Surg 2009;13:1831–8.
28. Kurman RJ, Shih Ie M. The origin and pathogenesis of epithelial ovarian cancer: a proposed unifying theory. Am J Surg Pathol 2010; 34:433–43.
29. Cejas P, Lopez-Gomez M, Aguayo C, Madero R, de Castro Carpeno J, Belda-Iniesta C, et al. KRAS mutations in primary colorectal cancer tumors and related metastases: a potential role in prediction of lung metastasis. PLoS One 2009;4:e8199.
30. Matsuo K, Lin YG, Roman LD, Sood AK. Overcoming platinum resistance in ovarian carcinoma. Expert Opin Investig Drugs 2010; 19:1339–54.
31. Lieu C, Kopetz S. The SRC family of protein tyrosine kinases: a new and promising target for colorectal cancer therapy. Clin Colorectal Cancer 2010;9:89–94.
32. Peterson-Roth E, Brdlik CM, Glazer PM. Src-induced cisplatin resistance mediated by cell-to-cell communication. Cancer Res 2009; 69:3619–24.
33. Pengetnze Y, Steed M, Roby KF, Terranova PF, Taylor CC. Src tyrosine kinase promotes survival and resistance to chemotherapeutics in a mouse ovarian cancer cell line. Biochem Biophys Res Commun 2003;309:377–83.
34. Schuh NR, Guerrero MS, Schrecengost RS, Bouton AH. BCAR3 regulates Src/p130 Cas association, Src kinase activity, and breast cancer adhesion signaling. J Biol Chem 2010;285:2309–17.

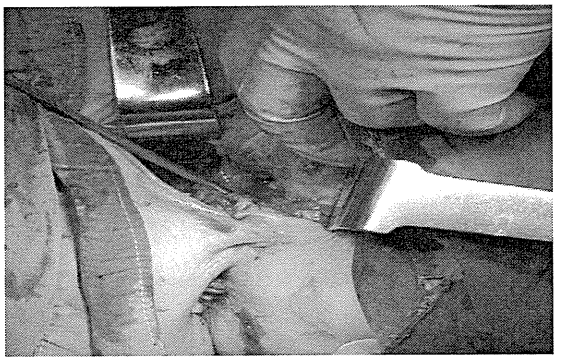

Fig. 1. Exploration of the abscess cavity.

Benassi et al. [2] reported a case of abscess formation at the ischiorectal fossa 7 months after TOT procedure, Goldman [3] described a patient with abscess formation in the region of gracilis and great adductor muscles. Robert et al. [4] reported case series of primary obturator abscess and mesh erosions after TOT procedures. They chose to drain the abscess vaginally and had good healing processes. Babalola et al. [5] reported an ischiorectal abscess following TOT procedure managed by gluteal drainage, which was healed nicely. In this patient, chronic paravaginal/ischiorectal abscess was observed and there may be the possibility of infection spreading from point of erosion in the vaginal wall to the obturator muscle region to the ischiorectal fossa. Longstanding drainage was managed by the help of gravity and walking through gluteal drain. We suggest that the chronic abscess formation may be due to recurrent urogynecological operations, previous unsuccessful vaginal route drainage procedures (proper time for drainage could not be allowed because of quick vaginal healing) and incomplete surgical removal of the tape (tape remainders formed a foreign body reaction and inflammation). Urogynecological procedures for stress urinary incontinence must be carefully selected and complete evaluation must be done before the recurrent operation. In an abscess formation, complete sling must be removed. We recommend our surgical technique for management of paravaginal, pararectal or ischiorectal abscess to avoid recurrences and for recurrent chronic abscess treatment.

References

[1] Deng DY, Rutman M, Raz S, Rodriguez LV. Presentation and management of major complications of midurethral slings: are complications under-reported? Neurourol Urodyn 2007;26:46–52.

[2] Benassi G, Marconi L, Accorsi F, Angeloni M, Benassi L. Abscess formation at the ischiorectal fossa 7 months after the application of a synthetic transobturator sling for stress urinary incontinence in a type II diabetic woman. Int Urogynecol J Pelvic Floor Dysfunct 2007;18:697–9.

[3] Goldman HB. Large thigh abscess after placement of synthetic transobturator sling. Int Urogynecol J Pelvic Floor Dysfunct 2006;17:295–6.

[4] Robert M, Murphy M, Birch C, Swaby C, Ross S. Five cases of tape erosion after transobturator surgery for urinary incontinence. Obstet Gynecol 2006;107:472–4.

[5] Babalola EO, Famuyide AO, McGuire LJ, Gebhart JB, Klingele CJ. Vaginal erosion, sinus formation, and ischiorectal abscess following transobturator tape: ObTape implantation. Int Urogynecol J Pelvic Floor Dysfunct 2006;17:418–21.

Ates Karateke
Zeynep Kamil Hospital, Pelvic Reconstructive Department, Istanbul, Turkey

Yesim Akdemir*
Zeynep Kamil Hospital, Pelvic Reconstructive Department, Murat Reis Mah, Bostanici Sok, Soyak Baglarbasi Evleri B10 D:11, 34664 Uskudar, Istanbul, Turkey

Mehmet Kucukbas
Sakarya Education and Training Hospital, Turkey

Hamdullah Sozen
Zeynep Kamil Hospital, Pelvic Reconstructive Department, Istanbul, Turkey

Cetin Cam
Zeynep Kamil Hospital, Pelvic Reconstructive Department, Uskudar, Istanbul, Turkey

*Corresponding author. Tel.: +90 5054970407
fax: +90 2163856463

E-mail addresses: karatekea@gmail.com (A. Karateke).
yesimakdemir@yahoo.com (Y. Akdemir).
kucukbas@yahoo.com (M. Kucukbas).
Hamdullah@gmail.com (H. Sozen).
camc@gmail.com (C. Cam).

26 January 2011

doi:10.1016/j.ejogrb.2011.04.045

A successful case of abdominal radical trachelectomy for cervical cancer during pregnancy

Dear Editor,

A 27-year-old woman (gravida 2, para 0) was referred to us due to cervical cancer at 12 weeks. The lesion was macroscopically visible. Pelvic MRI revealed a 20×7 mm cervical mass with minimal stromal invasion but no obvious metastasis to either pelvic lymph nodes or parametrial extension. A diagnosis of FIGO stage IB1 cervical cancer (squamous cell carcinoma) was made.

After extensive discussions, and obtaining written informed consent, we decided to perform abdominal radical trachelectomy (ART) during pregnancy, as previously reported by Ungar et al. [1], Mandic et al. [2], and Abu-Rustum et al. [3]. Surgery was performed at 15 weeks. To prevent abortion, 50 mg of an indomethacin rectal suppository was administered on the morning of the surgery; 25 mg more was administered immediately after surgery, and every 6 h thereafter, 4 times total. Also, 250 mg of 17-alpha-hdroxy-progesterone caproate was administered intramuscularly 60 min prior to surgery, and once a week thereafter, until 36 weeks of gestation.

Under general anesthesia with sevoflurane, the operation was initiated. Although the operative field was full with enlarged pregnant uterus, we were able to improve the operative field by displacing the uterus manually because indomethacin and sevoflurane were sufficiently effective at decreasing the tonus of the uterus. At first, pelvic lymphadenectomy was performed. By intraoperative pathology, negative for lymph node metastases were confirmed in bilateral obturator and external iliac nodes. Bilateral adnexae were preserved. After isolation of the left ureter from retroperitoneum, the left uterine artery was identified and gently dissociated from surrounding tissues. On the other hand, the right uterine artery was extremely thin and was unintentionally transected. After transection of anterior and posterior vesicouterine ligaments, cardinal ligaments were treated. Then uterosacral and rectovaginal ligaments were transected. The vaginal wall was cut from the 12 o'clock position circumferentially and then the cervix was transected 1 cm below the isthmus (Fig. 1). The excised specimen included 3.2 cm of uterine cervix with 1 cm of vaginal cuff. Margins were macroscopically clear; intraoperative

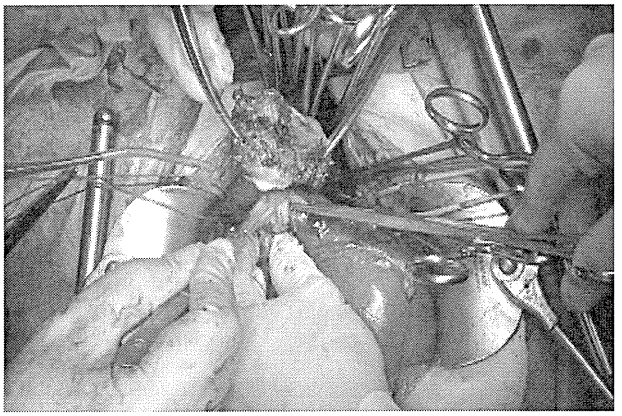

Fig. 1. In an abdominal radical trachelectomy during pregnancy at 15-weeks of gestation, the cervix was excised 1 cm below the isthmus.

frozen-section diagnosis confirmed negative margins. A Pap smear from remaining endocervix was negative. Semi-permanent cerclage was performed with nylon suture. The vaginal wall and remaining uterine cervix were anastomosed. Operation time was 7.5 h. Blood loss was 1200 ml; she received 960 ml of blood transfusion.

Microscopic vaginal invasion was observed in the anterior fornix. Final pathological diagnosis was squamous cell carcinoma of the uterine cervix, pT2a1, pN0, pM0; stromal invasion was less than 1/2; negative for margins; no apparent lymphovascular invasion. No metastases were detected in removed lymph nodes (0/16).

After the operation, we performed Pap smear every 4 weeks. Her pregnancy continued successfully, with normal Pap smear. Planned cesarean section was performed at 37 weeks. A healthy female infant was born weighing 2584 g, with an Apgar score 8/9. Currently, no sings of recurrence have been observed in the follow-up period of 6 months after the cesarean section.

First case of radical trachelectomy (vaginal) during pregnancy was reported by van de Nieuwenhof et al. in 2008 [4]. Since then, some cases have been reported although the indication and method are still not confirmed as standard procedure. ART at earlier weeks of gestation may seem favorable because the smaller uterus provides a better operative field. However, pregnancy outcome is poor when ART is performed during earlier weeks; in previous reports, 3 of 4 cases who underwent ART at less than 14 weeks resulted in intrauterine fetal death (IUFD) [1]. In addition, a single case of ART at 12 weeks resulted in IUFD during the surgery (personal communication, Dr. Tadayoshi Nagano, Kitano Hospital, Osaka, Japan). Meanwhile, 3 out of 4 cases who underwent surgery later than 15 weeks produced live infants [1–3,5]. Accordingly, we waited to perform ART at 15 weeks. Although we failed to preserve the right uterine artery, the surgery was completed without fetal loss; presumably collateral blood supply from the left uterine artery and both ovarian arteries maintained sufficient placental blood flow.

Similar experiences with this relatively new approach for cervical cancer in pregnant women should be accumulated and discussed widely to verify the strategy's safety and efficacy.

Disclosure statement

The authors declare that there are no potential conflicts of interest. A video file showing operative procedure is available direct from the authors.

Acknowledgments

The authors thank Dr. Masato Yamasaki for his technical supervision, Dr. Takuhei Yokoyama for surgical assistance, and Dr. Yoshiko Komoto and Dr. Masahiko Takemura for referring the patient.

References

[1] Ungar L, Smith JR, Palfalvi L, Del Priore G. Abdominal radical trachelectomy during pregnancy to preserve pregnancy and fertility. Obstet Gynecol 2006;108:811–4.
[2] Mandic A, Novakovic P, Nincic D, Zivaljevic M, Rajovic J. Radical abdominal trachelectomy in the 19th gestation week in patients with early invasive cervical carcinoma: case study and overview of literature. Am J Obstet Gynecol 2009;201:e6–8.
[3] Abu-Rustum NR, Tal MN, DeLair D, Shih K, Sonoda Y. Radical abdominal trachelectomy for stage IB1 cervical cancer at 15-week gestation. Gynecol Oncol 2010;116:151–2.
[4] van de Nieuwenhof HP, van Ham MA, Lotgering FK, Massuger LF. First case of vaginal radical trachelectomy in a pregnant patient. Int J Gynecol Cancer 2008;18:1381–5.
[5] Karateke A, Cam C, Celik C, et al. Radical trachelectomy in late pregnancy: is it an option? Eur J Obstet Gynecol Reprod Biol 2010;152:112–3.

Takayuki Enomoto
Kiyoshi Yoshino*
Masami Fujita
Yukari Miyoshi
Yutaka Ueda
Shinsuke Koyama
Toshihiro Kimura
Takuji Tomimatsu
Tadashi Kimura
Department of Obstetrics and Gynecology, Osaka University, Graduate School of Medicine, 2-2, Yamadaoka, Suita, Osaka 565-0871 Japan

*Corresponding author. Tel.: +81 66879 3355, fax: +81 66879 3359
E-mail address: yoshino@gyne.med.osaka-u.ac.jp (K. Yoshino).

18 February 2011

doi:10.1016/j.ejogrb.2011.04.048

sFlt-1 and PlGF levels in a patient with mirror syndrome related to cytomegalovirus infection

Dear Editor,

In 1892, John M. Ballantyne made the first description of tremendous maternal edema associated with fetal and placental hydrops due to rhesus alloimmunization [1]. In this syndrome the mother "mirrors" the general edema presented by compromised fetus and placenta [2]. Although the first Ballantine's report involved a patient with rhesus alloimmunization, other causes of fetal and placental hydrops have been associated with the disease, such as cytomegalovirus (CMV) and parvovirus B19 infections and twin-to-twin transfusion [3–5]. The complete pathogenesis of "mirror syndrome" is still not very clear, but some authors have recently described the involvement of an anti-angiogenic state [3,5]. Here, we describe a case of severe preeclampsia at 26 gestational weeks associated with massive placenta and fetal hydrops due to acute CMV infection. We found that increased concentrations of sFlt-1; (fms-like tyrosine kinase-1) are involved in the clinical syndrome manifested by patients with mirror syndrome.

A 23-year-old woman with a singleton pregnancy was referred to our university at 26 gestational weeks due to new-onset

Cancer Chemother Pharmacol (2011) 68:1603–1610
DOI 10.1007/s00280-011-1638-4

ORIGINAL ARTICLE

Chemotherapy for endometrial carcinoma (GOGO-EM1 study): TEC (paclitaxel, epirubicin, and carboplatin) is an effective remission-induction and adjuvant therapy

Tomomi Egawa-Takata · Yutaka Ueda · Chie Kuragaki · Takahito Miyake · Takashi Miyatake · Masami Fujita · Kiyoshi Yoshino · Ryuichi Nakashima · Mika Okazawa · Tateki Tsutsui · Ken-Ichirou Morishige · Tadashi Kimura · Masato Yamasaki · Takamichi Nishizaki · Masaaki Nagamatsu · Kimihiko Ito · Masahiro Asada · Kazuhide Ogita · Akinori Wakimoto · Toshiya Yamamoto · Yukihiro Nishio · Takayuki Enomoto

Received: 24 September 2010 / Accepted: 10 February 2011 / Published online: 17 May 2011

Abstract
Background TAP chemotherapy (paclitaxel, doxorubicin, and cisplatin) is effective for advanced and recurrent endometrial carcinoma, but has occasional severe toxicity. TEC chemotherapy (paclitaxel, epirubicin, and carboplatin) has been suggested to have less toxicity; however, the optimal dosage has yet to be determined.
Patients and methods Phase I/II prospective study for TEC therapy was performed. A retrospective comparison of the prognosis between adjuvant TEC therapy and radiation for completely resected cases with risk factors was also performed.
Results The recommended dose of TEC therapy was determined to be paclitaxel 150 mg/m^2, epirubicin 50 mg/m^2, and carboplatin AUC 4. A TEC regimen at this dose level was shown to be tolerable. The response rate and median overall survival were 74% and 37 months for those with advanced primary disease (Group B) and 50% and 26 months for recurrent tumors (Group C), respectively. A retrospective comparison showed that adjuvant TEC therapy for completely resected stage III cases improved their prognosis when compared to an adjuvant radiation therapy.
Conclusion TEC therapy was demonstrated to be a tolerable and effective treatment, not only as a remission-induction

Electronic supplementary material The online version of this article (doi:10.1007/s00280-011-1638-4) contains supplementary material, which is available to authorized users.

T. Egawa-Takata · Y. Ueda · C. Kuragaki · T. Miyake · T. Miyatake · M. Fujita · K. Yoshino · R. Nakashima · M. Okazawa · T. Tsutsui · K.-I. Morishige · T. Kimura · T. Enomoto (✉)
Department of Obstetrics and Gynecology,
Osaka University Graduate School of Medicine,
2-2, Yamadaoka, Suita, Osaka 565-0871, Japan
e-mail: enomoto@gyne.med.osaka-u.ac.jp

T. Miyake · M. Yamasaki
Osaka Rosai Hospital, 1179-3 Kita-ku Nagasone-cho,
Sakai, Osaka 591-8025, Japan

M. Okazawa · M. Nagamatsu
Kaizuka City Hospital, 3-10-20 Hori, Kaizuka,
Osaka 597-0015, Japan

T. Nishizaki
Suita Municipal Hospital, 2-13-20 Katayama-cho,
Suita, Osaka 564-0082, Japan

K. Ito
Kansai Rosai Hospital, 3-1-69 Inabaso, Amagasaki,
Hyogo 660-8511, Japan

M. Asada
Itami City Hospital, 1-100 Koyaike, Itami,
Hyogo 664-8540, Japan

K. Ogita
Rinku General Medical Center, 2-23 Rinku Orai-kita, Izumisano,
Osaka 598-8577, Japan

A. Wakimoto
Osaka Koseinenkin Hospital, 4-2-78 Fukushima, Fukushima-ku,
Osaka 553-0003, Japan

T. Yamamoto
Sakai Municipal Hospital, 1-1-1 Sakai-ku Minami Yasui-cho,
Osaka 590-0064, Japan

Y. Nishio
Osaka Police Hospital, 10-31 Kitayama-cho, Tennoji-ku,
Osaka 543-0035, Japan

therapy for advanced and recurrent endometrial carcinomas but also as the adjuvant therapy.

Keywords Endometrial cancer · Combination chemotherapy · TEC · Paclitaxel · Epirubicin · Carboplatin

Abbreviations

CAP	Cisplatin, adriamycin, and cyclophosphamide
TAP or AP	Doxorubicin and cisplatin (with or without paclitaxel)
TC or TEC	Paclitaxel and carboplatin (without or with epirubicin)
TEP	Paclitaxel, epirubicin, and cisplatin
ALT	Alanine aminotransferase
AST	Aspartate aminotransferase
AUC	Area under the plasma drug concentration versus time curve
CR	Complete response
DLT	Dose limiting toxicity
FIGO	International Federation of Gynecology and Obstetrics
G-CSF	Granulocyte-colony stimulating factor
GOG	The gynecologic oncology group
GOGO	The gynecologic oncology group of Osaka
Gy	Gray, unit of absorbed radiation
MTD	Maximum tolerated dose
OS	Overall survival
PD	Progressive disease
PFS	Progression-free survival
PR	Partial response
RR	Responsive rate
RT	Radiation therapy
SD	Stable disease
WAI	Whole-abdominal radiation therapy
WBC	White blood cells
5-HT_3	5-hydroxytriptamine-3

Introduction

Endometrial cancer is the most common gynecological cancer in the Western world. Although its incidence has increased during the last three decades, its treatment has also evolved considerably during the same period. Surgical therapy currently consists of hysterectomy, bilateral salpingo-oophorectomy, and retroperitoneal lymph node dissection. Prognostic factors for the disease include histological type and differentiation, stage, level of myometrial invasion, peritoneal cytology, lymph node metastasis, and adnexal metastasis [1, 2].

In the past, patients with poor prognostic factors usually underwent adjuvant post-operative irradiation. Recently, a randomized study by the Gynecologic Oncology Group (GOG #122) revealed that a combined chemotherapy of AP (doxorubicin 60 mg/m^2 and cisplatin 50 mg/m^2) was superior to whole abdominal irradiation (45 Gy WAI) as the adjuvant therapy. However, significant hematologic and cardiac toxicity and treatment-related death were detected in the chemotherapy arm of the AP study [3].

Recently, a randomized study showed a better response rate and longer progression-free and overall survival rates (PFS and OS) using TAP (a combination of paclitaxel (160 mg/m^2), doxorubicin (45 mg/m^2), and cisplatin (50 mg/m^2)) than with AP (GOG #177) [4]. However, the neurologic toxicity was even worse for the patients receiving TAP, with 39% suffering grade 2–3 peripheral neuropathy, compared with 5% of those in the group receiving AP. Three patients (2%) on the TAP arm, versus none on AP arm, developed grade 3 heart failure, and treatment-related death occurred in five patients (4%) on the TAP arm, versus none with AP. Thus, the TAP regimen is often avoided because of its toxicity, despite its proven better effectiveness for advanced and recurrent endometrial cancer. GOG is currently running a study to compare the combination of paclitaxel and carboplatin (TC) with TAP.

Lissoni et al. reported that TEP (a combination of paclitaxel 175 mg/m^2, epirubicin 70 mg/m^2, and cisplatin 50 mg/m^2) exhibited high anti-tumor activity against advanced endometrial carcinoma and good tolerability [5]. The TEP response rate for advanced endometrial carcinoma was 73%; however, grade 3–4 neutropenia occurred in 61% of the recipients, with possibly one related death.

More recently, TEC, a combination of paclitaxel (150 mg/m^2), epirubicin (50 mg/m^2), and carboplatin (AUC 5), when combined with G-CSF support, was shown to be potently active against metastatic and recurrent endometrial carcinomas. This TEC treatment was accompanied by grade 3–4 neutropenia in 15.5% and grade 2–3 neurotoxicity in 19% of patients [6]. However, a determination of the proper dosage for the TEC regimen was not performed, and its effectiveness as an adjuvant therapy remains to be clarified.

In our phase I/II prospective study being described here, we first determined the optimal dose for TEC therapy; subsequently, we analyzed the safety and responsiveness to the regimen for advanced or recurrent endometrial carcinomas. Moreover, we studied the effectiveness of our TEC regimen as an adjuvant therapy for optimally resected endometrial cancer with risk factors of recurrence.

Materials and methods

This study was conducted during the period of 1999–2007 by the Gynecologic Oncology Group of Osaka (GOGO)

that included Osaka University Hospital, Osaka Rosai Hospital, Kaizuka City Hospital, Suita Municipal Hospital, Kansai Rosai Hospital, Itami City Hospital, Osaka Kouseinenkin Hospital, Rinku General Medical Center, Sakai Municipal Hospital, and Osaka Police Hospital.

Eligibility

Participation eligibility required that the patient have adequate hematologic findings (WBC $\geq$ 3,000/μl, platelets $\geq$ 100,000/μl, granulocytes $\geq$ 1,500/μl, and hemoglobin $\geq$ 10 g/dl), and renal (creatinine $\leq$ 2 mg/dl) and hepatic (bilirubin $\leq$ 3 mg/dl, AST and ALT $\leq 2\times$ the institutional normal value) functions. A relative performance status of 0–2 was needed. The tumors needed to be histologically diagnosed as being a primary or recurrent endometrial carcinoma. The age of the patients needed to be 70 years of age or less, and the patient needed to have an estimated remaining survival time of greater than 3 months. Those with synchronous cancers or with serious concomitant medical illnesses were deemed ineligible. All patients provided voluntary written informed consent before the treatment commenced.

Phase I component

Adverse treatment effects were graded based on WHO criteria for toxicity. For our phase I study of TEC therapy, the maximum tolerated dose (MTD) levels of paclitaxel, epirubicin, and carboplatin were evaluated. The drugs were administered every 3–4 weeks for 3–6 cycles. The starting dose was set at 150 mg/m^2 for paclitaxel, 50 mg/m^2 for epirubicin, and AUC 4 for carboplatin. G-CSF (granulocyte colony-stimulating factor) was used to support hematopoiesis when grade 4 neutropenia, or grade 3 neutropenia with fever, was observed.

A 3 + 3 study design was used for dose escalation. The first and second dose escalation indicated an AUC of 4.5 to 5 for carboplatin, the third escalation found 175 mg/m^2 for paclitaxel, and the fourth escalation was 70 mg/m^2 for epirubicin. The first reduction indicated 30 mg/m^2 for epirubicin, the second indicated 135 mg/m^2 for paclitaxel, and the third indicated AUC 3.5 for carboplatin. Dose limiting toxicity (DLT) was defined as when grade-4 hematologic toxicity and grade-3 non-hematologic toxicity occurred. MTD indicated the highest dose level at which $\leq$33% of patients ($\leq$2 of 6 patients) experienced a DLT, and the recommended phase II dose was the MTD, as previously described [7].

Phase II component

For our phase II study, the patients were divided into three groups. The patients with no residual tumor larger than 1 cm after surgery, but who still had a significant risk for a recurrence, were placed in Group A. Surgery typically consisted of a total abdominal hysterectomy, bilateral salpingo-oophorectomy, and a lymphadenectomy for staging. Lymphadenectomy was omitted when the histology was diagnosed as grade-1 endometrioid adenocarcinoma without invasion of the myometrium. Cytoreductive surgery was added as needed. The considerations for assigning a high risk for a recurrence included being FIGO (International Federation of Gynecology and Obstetrics) stage III or IV, a myometrium invasion of >1/2, or a special type of histology, such as endometrioid adenocarcinoma grade 3, clear cell carcinoma, uterine serous papillary carcinoma, or carcinosarcoma.

The stage IIIa patients who had only a positive peritoneal cytology and none of the other risk factors described above were not included. Treatment was repeated every 3–4 weeks and continued for 3 or 6 cycles until disease progression or unacceptable toxicity. Stage III or IV patients or recurrent disease was planned to receive 6 cycles of TEC therapy. Patients with other risks were planned to receive 3 cycles of the therapy.

Patients who had a measurable tumor with CT larger than 1 cm remaining after cytoreductive surgery were combined with patients who received primary TEC therapy for an inoperable tumor as Group B. Patients suffering from a recurrent disease were defined as Group C. In Group C, 9 patients received surgery and adjuvant radiation, and one patient underwent surgery alone, with no follow-up adjuvant. Our study patients' characteristics are listed in Table 1. Patients in Group A were treated with TEC at the phase II dose determined in our phase I study. Any and all patients who received TEC therapy at the same dose as the recommended phase II dose were included in our study.

The primary endpoints of the phase II trial were the toxicity of TEC regimen and the clinical response for the patients with advanced (Group B) and recurrent (Group C) endometrial cancer.

The secondary endpoints of our phase II study were the progression-free survival and overall survival. We used RECIST (version 1.0, response evaluation criteria in solid tumors) for evaluating the therapy response. A complete response (CR) required regression of all tumors. A partial response (PR) required >30% reduction in the sum of the largest diameter of the target legions. A progressive disease (PD) means that new lesions appeared, or the sum of the largest diameter of the target lesions enlarged >20%. All other diseases were considered to be a stable disease (SD).

Progression-free survival (PFS) and overall survival (OS) of the three groups were evaluated over a median follow-up period of 36 and 37 months for Group A, 12 and 26 months for Group B, and 6 and 18 months for Group C, respectively.